European Journal of Pharmaceutical Sciences 115 (2018) 296–303

Contents lists available at ScienceDirect

European Journal of Pharmaceutical Sciences

journal homepage: www.elsevier.com/locate/ejps

# Predicting tumour growth and its impact on survival in gemcitabine-treated patients with advanced pancreatic cancer

Maria Garcia-Cremades[a,b,1], Celine Pitou[c], Philip W. Iversen[d], Iñaki F. Troconiz[a,b,*]

[a] Pharmacometrics and Systems Pharmacology, Department of Pharmacy and Pharmaceutical Technology, School of Pharmacy, University of Navarra, Pamplona, Spain
[b] Navarra Institute for Health Research (IdiSNA), University of Navarra, Pamplona, Spain
[c] Global Pharmacokinetic/Pharmacodynamics and Pharmacometrics, Eli Lilly and Company Windlesham, Surrey, United Kingdom
[d] Lilly Research laboratories, Eli Lilly and Company, Indianapolis, Indiana, USA

ARTICLE INFO

*Keywords:*
PKPD
Tumour
Survival
Gemcitabine
MID3

ABSTRACT

The aim of this evaluation was to characterize the impact of the tumour size (TS) effects driven by the anticancer drug gemcitabine on overall survival (OS) in patients with advanced pancreatic cancer by building and validating a predictive semi-mechanistic joint TS-OS model.

TS and OS data were obtained from one phase II and one phase III study where gemcitabine was administered (1000-1250 mg/kg over 30-60 min i.v infusion) as single agent to patients ($n$ = 285) with advanced pancreatic cancer. Drug exposure, TS and OS were linked using the population approach with NONMEM 7.3.

Pancreatic tumour progression was characterized by exponential growth (doubling time = 67 weeks), and tumour response to treatment was described as a function of the weekly area under the gemcitabine triphosphate concentration vs time curve (AUC), including treatment-related resistance development. The typical predicted percentage of tumour growth inhibition with respect to no treatment was 22.3% at the end of 6 chemotherapy cycles. Emerging resistance elicited a 57% decrease in drug effects during the 6th chemotherapy cycle. Predicted TS profile was identified as main prognostic factor of OS, with tumours responders' profiles improving median OS by 30 weeks compared to stable-disease TS profiles. Results of NCT00574275 trial were predicted using this modelling framework, thereby validating the approach as a prediction tool in clinical development.

Our analyses show that despite the advanced stage of the disease in this patient population, the modelling framework herein can be used to predict the likelihood of treatment success using early clinical data.

## 1. Introduction

Currently pancreatic cancer constitutes one of the most aggressive and lethal oncology diseases (Schober et al., 2015; Perkhofer et al., 2014). Prognosis is particularly poor with an overall 5-year survival rate of < 5% and a median survival of 6 months when patients are not treated (Le et al., 2016). The potential cure for these patients is limited to surgery and this is only feasible at early stages of the malignancy, when the tumour is still resectable. However, only around 10-20% of patients present with resectable disease, and, even in this situation, only around 20% survive up to 5 years (Neoptolemos et al., 2004). Over the years, limited advances have been made in the treatment of pancreatic cancer, with very few anticancer drugs found to bring any real benefit. The first cytotoxic drug that was shown to produce a meaningful impact on survival and disease-related symptoms in pancreatic adenocarcinoma was gemcitabine (Moore, 1996; Oettle et al., 2000).

Gemcitabine is a nucleoside antimetabolite anticancer pro-drug, indicated for the treatment of multiple types of cancer (Oettle et al., 2000; Toschi et al., 2005). The parent compound requires cellular uptake and intracellular phosphorylation to achieve its active form (gemcitabine triphosphate) in order to exert its cytotoxic action (Mini et al., 2006).

The standard dosing schedule used in clinic (30 min i.v infusion of 1000 mg/m2 given weekly for 3 weeks followed by 1 week rest (Toschi et al., 2005; Zhang et al., 2006) has proved to be useful for prolonging survival and alleviating the symptoms of patients with advanced pancreatic cancer (Moore, 1996). However, the life expectancy of such patients is still discouraging, with an overall survival of 7.2 months and an objective response rate to treatment of only 10% (Fuchs et al., 2015). Moreover, apart from the highly variable nature of response rates

* Corresponding author at: Pharmacometrics & Systems Pharmacology, Department of Pharmacy and Pharmaceutical Technology, School of Pharmacy, University of Navarra, Pamplona 31008, Spain.
*E-mail addresses:* mgarcia-cre@alumni.unav.es (M. Garcia-Cremades), pitou_celine@lilly.com (C. Pitou), iversen_philip_w@lilly.com (P.W. Iversen), itroconiz@unav.es (I.F. Troconiz).
[1] Present address: Dept. Bioengineering, UC San Francisco, San Francisco, California. USA

https://doi.org/10.1016/j.ejps.2018.01.033
Received 10 October 2017; Received in revised form 17 January 2018; Accepted 18 January 2018
Available online 31 January 2018
0928-0987/ 

(Ciccolini et al., 2016) an even more important limitation is that the majority of patients develop resistances to the drug (Bergman et al., 2002).

Although new therapeutic strategies are emerging for pancreatic cancer (Perkhofer et al., 2014), treatment with gemcitabine still constitutes the first line therapy, either given in combination with nab-paclitaxel for patients with ECOG status 0-1, or as a single agent for advanced patients (ECOG > 1) (Ruess et al., 2017), and for those patients who cannot receive the combination treatments.

The paradigm of linking drug exposure and clinical endpoints through the incorporation of bio-/surrogate markers in a quantitative framework has been successfully applied in oncology, during a decade of efforts (Bender et al., 2015).These modelling efforts have allowed to identify metrics (such as the change of tumour size at a specific time point after the start of treatment) predicting overall survival (OS) (Claret et al., 2009; Wang et al., 2009), with important application in drug development and clinical use of anti-cancer drugs. Previous works have contributed to the understanding of tumour progression dynamics using computational models (Menze et al., 2011; Konukoglu et al., 2010; Hogea et al., 2008; Chen et al., 2013; Liu et al., 2014).

Gemcitabine effects have been described under the model-based paradigm mentioned above for non-small cell lung cancer (NSCLC), metastatic ovarian cancer and metastatic breast cancer (Tham et al., 2008; Zecchin et al., 2016; Tate et al., 2016). In all these evaluations gemcitabine was given in combination with carboplatin (Tham et al., 2008; Zecchin et al., 2016) and with paclitaxel (Tate et al., 2016). With respect to pancreatic cancer, a model linking tumour size (TS) with OS has been recently published (Wendling et al., 2016). However, drug exposure information was not reported (i.e., dose levels, treatment duration or dose reductions or discontinuations) thus precluding the characterization of gemcitabine effects and limiting the use of the model to evaluate outcome results from model-based simulations exploring alternative dosing scenarios. In addition, ignoring drug exposure prevents analysis of whether progression in the disease occurs due to treatment interruptions or emerging resistance.

Based on the above considerations, the main objective of this evaluation was to build a joint TS and OS population pharmacokinetic/pharmacodynamics (PKPD) model of gemcitabine in patients with advanced pancreatic cancer including the time course of drug exposure and its effect on TS. During the course of this analysis the contribution of TS over time as a driver of OS was evaluated beyond statistical significance. In addition, and due to the fact that, at least to the best of our knowledge, most models linking drug exposure, TS and OS have not been externally validated, we aimed to confirm the robustness of our approach challenging the current model against results reported from other clinical studies.

## 2. Methods

### 2.1. Data and studies design

Data were obtained from two clinical studies in phase II (study JEAL; NCT00055250) and III (study JMES; NCT00035035) in which previously untreated patients with locally advanced or metastatic pancreatic cancer were treated with gemcitabine. The primary endpoint of both studies was OS. Secondary endpoints included tumour response rate, progression free survival, or time to response among others. In the JEAL study, patients were treated with the current standard treatment, receiving an i.v infusion (over 30–60 min) of 1000 mg/m$^2$ of gemcitabine in a 28-day cycle of treatment (given on days 1, 8 and 15). In the JMES study, gemcitabine was given intravenously (during 30–60 min) at the dose of 1250 mg/m$^2$ in a 21 day-cycle (given on days 1 and 8). Dose adjustments were based on the absolute neutrophil and platelet counts measured on the corresponding day of therapy. For both studies, the planned duration of treatment, in the absence of disease progression, was up to 6 cycles of gemcitabine. Nevertheless, patients could continue receiving cycles in case of benefit. Treatment could also be discontinued and patients dropped from the studies mainly due to (i) progressive disease, (ii) unacceptable toxicity and (iii) patient or investigator decision. Even when such exclusions occurred, TS measurement and patient status were assessed every three months until death. Details of patient characteristics at the beginning of the studies can be found in Supplementary Table S1.

A CT (computerized tomography) (80% of patients), MRI (magnetic resonance imaging) (4% of patients) or spiral CT (16% of patients) scan was routinely repeated before drug administration at every cycle, and the sum of the longest diameters for all target lesions was calculated and reported, assuming that all the tumour lesions were identified.

Written informed consent was obtained from all patients or their legally authorized representatives, prior to the performance of any protocol-specific procedures. Studies were conducted in accordance with the ethical principles outlined in the Declaration of Helsinki, consistent with good clinical practices and the applicable laws and regulations, and were approved by the institutional review board of the ethics committee at each study site.

### 2.2. Data analysis

Data from both studies were pooled, and in total data from 285 patients (58 of phase II & 227 of phase III) were analysed.

Pharmacokinetic, TS and OS data were linked and described based on the population approach with NONMEM 7.3 (Bauer, 2011) using the LAPLACE estimation method with the INTERACTION option. TS data were logarithmically transformed for the analysis. Inter-subject variability (ISV) was modelled exponentially, and the residual error for TS was described with an additive error model on the logarithmic domain of the transformed data. OS information was treated as a right-hand censored time to event variable.

### 2.3. Gemcitabine pharmacokinetics

The weekly area under the gemcitabine triphosphate concentration vs time curve in white blood cells (AUC), was predicted for each dose administration based on the individual dosing history (including dose reductions and delays in treatment administrations) and a pharmacokinetic model of gemcitabine developed previously (Zhang et al., 2006), describing the formation of gemcitabine triphosphate which occurs intracellularly following a saturable mechanism, was also used. The covariate relationships between body surface area, gender and age, and total clearance identified in the mentioned model (Zhang et al., 2006) was considered in the prediction of the AUC.

### 2.4. Tumour growth inhibition model

TS comprised the sum of the longest diameters (SLD) of every lesion in every organ. New lesions were also considered and their SLD added to TS. TS was characterized as the result of a balance between the processes of tumour cell proliferation and drug-induced tumour shrinkage, and shown in Eq. 1:

$$dTS/dt = Kp \times TS - E_{drug} \times TS \quad (1)$$

TS proliferation was characterized by the first order rate constant $Kp$. The term $E_{drug}$ represents drug effects and is composed of two terms, one accounting for drug efficacy of the form Slope × AUC and the other reflecting resistance to treatment as described in Eq. 2, where $R_2$ accounts for the decrease in drug effects due to exposure to treatment. $TS_0$, the value of TS at the beginning of each of the studies, corresponds to the initial condition of the system described by Eq. 1.

$$E_{drug} = Slope \times AUC/(1 + R_2) \quad (2)$$

The set of Eqs. 3 and 4 quantifies the dynamics of the resistance phenomena, characterized by the first order rate constant $K_R$, where $R_1$

and $R_2$ represent two transit compartments included in the model to delay the development of the resistance mechanisms with respect the presence of gemcitabine triphosphate in plasma.

$$dR_1/dt = K_R \times (AUC - R_1) \quad (3)$$

$$dR_2/dt = K_R \times (R_1 - R_2) \quad (4)$$

The resistance model described in Eqs. 3 and 4 implies that resistance is reversible. That and other underlying assumptions included in the model for TS were tested as part of the model building process as shown in Supplementary Table S2, where a summary of the key models and an overview of corresponding results are presented.

### 2.5. Overall survival

A parametric time-to-event model was used to describe OS. Different distributions (exponential, Gompertz and Weibull) were explored to characterize the hazard rate (*hz*). Eq. 5 represents the model corresponding to the Weibull distribution.

$$hz = \lambda \times \beta \times (\lambda \times t)^{\beta-1} \quad (5)$$

Where λ and $\beta$ are the base and shape parameters of the Weibull distribution model. The link between *hz* and OS is established through the cumulative hazard (*HZ*) as indicated by the following expression: $OS = e^{-HZ}$ (Collett, 1952).

### 2.6. Model selection

Models were selected based on the (i) minimum value of the objective function provided by NONMEM, which is approximately equal to −2 log (likelihood) (−2LL) where a decrease in -2LL of 3.84, 6.63 and 10.83 points between two nested models is considered significant at *p* values of 0.05, 0.01 and 0.001, respectively, (ii) visual exploratory analysis of the goodness of fit plots and predictive checks and (iii) meaningfulness of the parameter estimates, as well as their precision.

### 2.7. Covariate analysis and selection

Once the joint model for TS inhibition and OS was developed, a covariate analysis was performed. The following patient's characteristics measured at baseline were taken into account for inclusion in the model: Number of organs damaged with tumour lesions (NODB), number of tumour lesions (NLSB), tumour lesion location, disease stage, and ECOG status. These covariates were tested on the $TS_0$, *Kp*, *Slope*, λ and $\beta TS_0$ parameters.

Selected covariates were finally included following the general covariate model described in Eq. 6:

$$TVP = \theta_n \times \prod_1^m \left(\frac{cov_m}{cov_{m,ref}}\right)^{\theta_m} \times \prod_1^p \theta_{p,ctg} \quad (6)$$

TVP represents the typical value of a model parameter and is described as a function of *m* continuous ($cov_m$) and *p* categorical covariates. For each p covariate, $\theta_{p,ctg}$ takes the value of 1 for one of the categories (ctg), usually the most common within the studied population, and for the rest of the categories, the corresponding parameter estimates. $\theta_n$describes the $n^{th}$ typical parameter value for an individual with covariate values ($cov_m$) equal to the reference values: [($cov_m = cov_{m,ref}$) and ($\theta_{p,ctg} = 1$)]. $cov_{m,ref}$ refers to the median value across the populations studied. $\theta_m$ is the parameter quantifying the magnitude of the continuous covariate-parameter relationship.

Covariate selection was performed using the stepwise covariate modelling implemented in the PsN software (v4.48) (Lindbom et al., 2004) by means of the −2LL ratio test with significance levels of 0.01 and 0.001 for the forward inclusion and for backward deletion approaches, respectively.

### 2.8. Model evaluation

TS and OS models were evaluated through simulation-based diagnostics, performing Visual Predictive Checks (VPCs) (Bergstrand et al., 2011; Nyberg et al., 2014). In addition, the precision of the parameter estimates was evaluated from the analysis of 500 simulated bootstrap datasets. The condition of over-fitting was also explored fitting the selected model to two subsets of the original dataset, containing data from 25% and 75% of the total of patients, respectively.

### 2.9. External model validation

The model was externally validated with the TS model and the OS data published by Wendling et al. (Wendling et al., 2016) using VPCs. As no raw TS data over time were available, 500 TS profiles were simulated using Wendling's model, and used as the external data for validation purposes. We then generated VPCs by simulating 500 replicate datasets with the same characteristics as those of the external dataset (i.e, dosing schedule, $TS_0$ and covariate information) using the currently developed model. For the validation of the OS model, survival profiles obtained from 500 hundred studies simulated with the study conditions reported by Wendling and the current model, were summarized as a Kaplan Meier plot represented by the 95% confidence intervals and compared with the raw OS shown in Wendling et al. (Wendling et al., 2016).

### 2.10. Model exploration

One of the main objectives of the current evaluation was to study whether or not TS in advanced pancreatic cancer proves to be a relevant predictor of OS. To evaluate the impact of TS on OS beyond statistical significance, we performed the following simulation exercise: (i) First, TS profiles were simulated for two hundred patients receiving the standard dosing schedule of gemcitabine (i.v infusion (over 30–60 min) of 1000 mg/m$^2$ of gemcitabine in a 28-day cycle of treatment (given on days 1, 8 and 15)), then (ii) three individual simulated profiles, below the 2.5th percentile, similar to the 50th percentile, and above the 97.5 percentile of the simulated distribution, representing tumour response, stable tumour profile and tumour progression, respectively, were selected; (iii) Finally, for each of the selected TS profiles, 200 OS profiles were generated and compared visually.

The Perl-speaks-Nonmem (PsN v4.48), R (version 3.2.0), Simulx (http://simulx.webpopix.org/), Berkeley Madonna (version 8.3.18), and NONMEM 7.3 software were used to perform the required calculations for the bootstrap analysis, VPC, simulation exercises and graphical representation.

## 3. Results

### 3.1. General description of the data

Raw data are shown in Fig. 1A. When looking at the whole range of TS observations, it is difficult to observe a general trend in the data. However, when tumour profiles are observed individually, a slight response to the treatment, followed by tumour relapse during the treatment period can be observed. Some examples of these profiles are highlighted in red and displayed in Fig. 1A (left panel). In total, 904 TS measurements were analysed. 51% of the patients already presented metastasis at baseline in one or more organs, mostly in the liver (54%). Regarding OS, patients died during the course of study (Fig. 1A, right panel), with the median survival being about 33 weeks.

### 3.2. Joint tumour growth inhibition and survival model

The schematic representation of the selected model for the tumour shrinkage effects of gemcitabine and its impact on OS is represented in

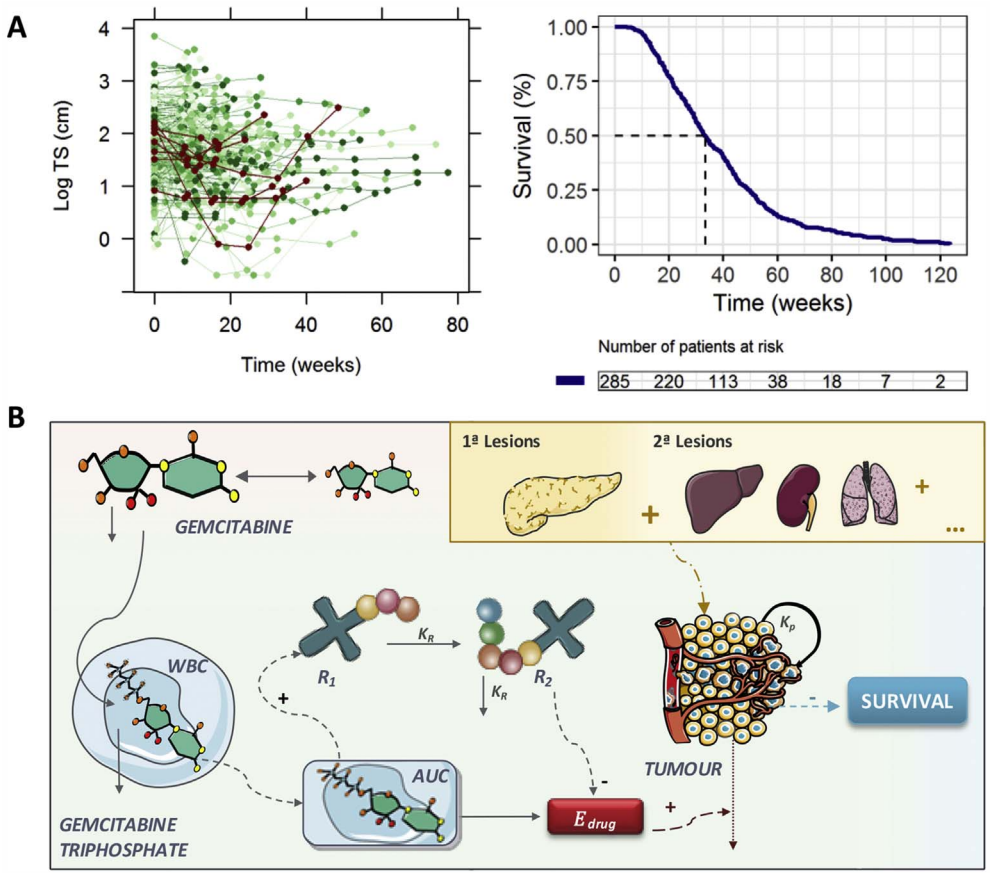


**Fig. 1.** Raw data & schematic representation of the model. A. In the left panel, TS profiles are represented over time in a logarithmic scale, where a few individual profiles are highlighted in red. The panel in the right corresponds to the Kaplan Meier plot showing the time profile of the OS probability, highlighting the median survival time and including the number of patients at risk during time. B. The green molecular structure corresponds to gemcitabine. WBC represents the development and accumulation of gemcitabine triphosphate in white blast cells. A description of the rest of terms and model parameters can be found in the Patients and Methods section. (For interpretation of the references to colour in this figure legend, the reader is referred to the web version of this article.)

Fig. 1B. An exponential growth model best described the natural progression of the disease. The model predicted a time of a 100% increase in TS with respect to baseline of 67 weeks. Tumour response to treatment was best described ($p < 0.001$) by the predicted AUC of gemcitabine triphosphate compared to the results using AUC corresponding to the parent drug. The individual predicted TS profiles shown in Fig. 2A represent at least three different behaviours: (i) responders, (ii) non-responders, and (iii) initial response to treatment followed by a relapse, which was well captured by the resistance term incorporated into drug effects.

As described in the methods section, the probability of OS in advanced pancreatic cancer was well described by a parametric survival model using the Weibull distribution. The impact of TS profile on OS was evaluated and proved significant ($p < 0.001$). Eq. 7 describes the model for the hazard rate selected where the term $e^{\gamma \times Log(TS)}$ describes the change in *hz* elicited by TS.

$$hz = \lambda \times \beta \times (\lambda \times t)^{\beta-1} \times e^{\gamma \times Log(TS)} \quad (7)$$

Among the covariates tested, NLSB and NODB were found to have a significant impact ($P < 0.001$) on $TS_0$. With respect to OS, ECOG was the only covariate that showed statistical significance ($P < 0.001$) on the $\beta$ parameter.

Table 1 lists the estimates of model parameters associated with their measures of precision corresponding to the final joint TS and OS model. With respect to parameter precision, the 95% confidence intervals (computed from the bootstrap analysis) of any of the parameters include the value of zero, indicating that the data analysed supported the degree of complexity of the model selected. A moderate 40% ISV in $TS_0$ was obtained. Estimates of ISV corresponding to *Kp* and *Slope* were higher (87% and 86%, respectively). Supplementary Table S3 displays the parameter estimates obtained from the analysis of the two data subsets. All estimates show consistency across datasets as their values are covered by the 95% confidence intervals obtained from the original complete dataset. The selected model showed good performance at the individual level as can be seen in Fig. 2A, where several individual TS profiles are displayed with their corresponding model predictions. Fig. 2B and C show the VPCs corresponding to TS and OS, respectively, demonstrating good agreement between observed and simulated data. For TS, the dispersion at times > 30 weeks appears to be over-predicted. However it should be taken into consideration that at those later times, the number of patients remaining in the study decreased considerably.

The results from the external validation of the model are shown in Fig. 3. Remarkably, the current model describes quite well the simulated data based on the model structure and parameters provided by Wendling et al. (Wendling et al., 2016) for the case of both response outcomes, TS and OS.

The design and patient population characteristics between training and validation clinical trials are shown in Supplementary Table S1.

Fig. 4 displays the contribution of TS as a predictor of OS. The results from the simulation exercise indicate there is no overlap in the 95% prediction intervals in OS between patients exhibiting disease progression and those showing stable disease and a partial response. However, for partial and non-responders, although the graph shows a clear distinction between the median profiles, the corresponding 95% prediction intervals overlap slightly at initial times.

Fig. 5A shows the impact of the selected covariates, ECOG, NODB and NLSB on the OS through deterministic simulations. The results displayed suggest no major impact of the above listed covariates. In Fig. 5B,C the effect of resistance on TS profiles and $E_{drug}$ is explored, respectively, calculating different metrics (see below) derived from the TS profile of an untreated patient and two patients receiving six chemotherapy cycles of the standard treatment of gemcitabine (1000 mg/m2 iv, 30 min infusion, administered weekly ×3 followed by a week of

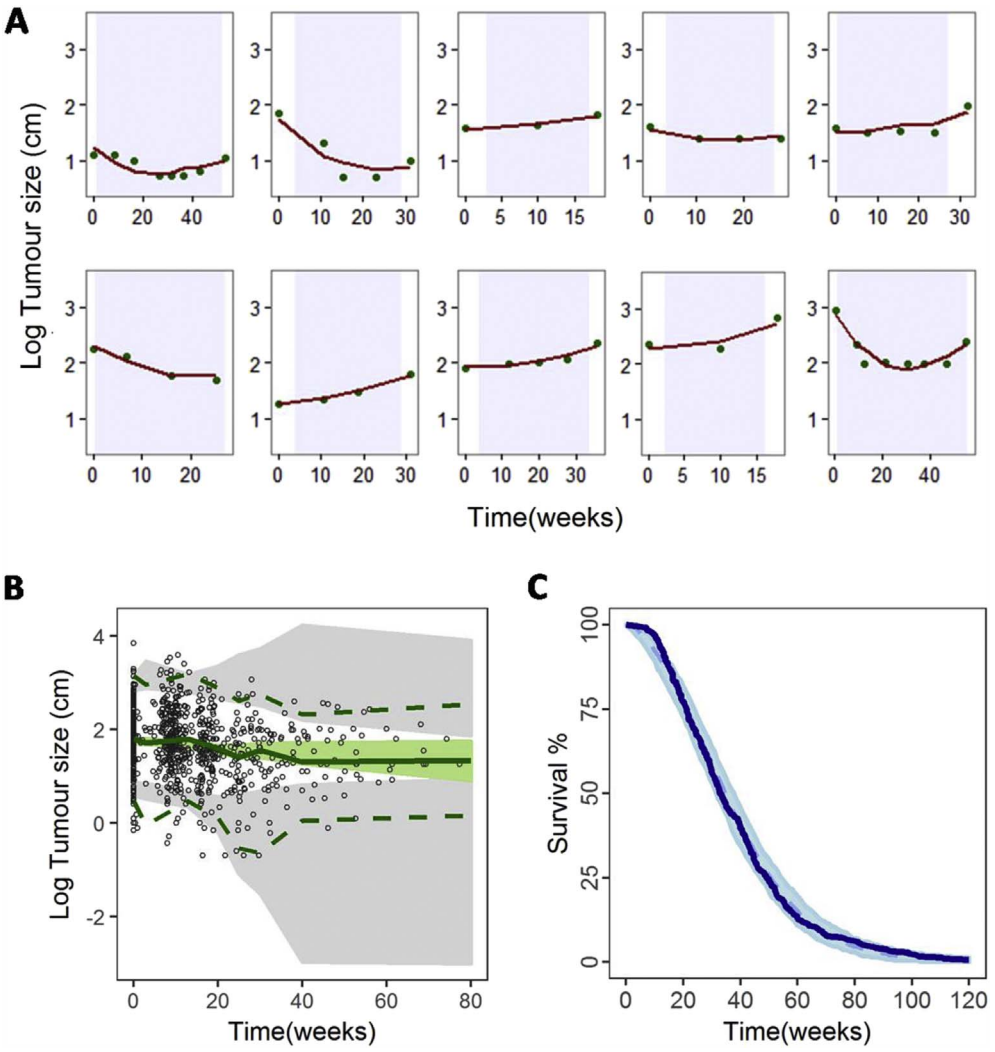


**Fig. 2.** Model evaluation. A. Individual TS observations (green points) and model predictions (red lines) in logarithmic scale vs time from a set of patients selected at random. Vertical grey areas represent duration of treatment. B. Visual predictive checks corresponding to the selected TS model. Dots represent the TS observations; the solid green line corresponds to the 50th percentile of the observations while the dashed green lines represent the 5th and 95th percentiles of these observations. Shaded green and grey areas are the 95% predicted intervals for the median, 5th and 95th percentiles obtained from 500 simulated datasets. C. Kaplan Meier plot of OS probability. The solid blue line represents raw data while the blue shaded area cover the 95% prediction interval calculated from the 500 simulated studies. (For interpretation of the references to colour in this figure legend, the reader is referred to the web version of this article.)

**Table 1**
Population Parameters Estimates.

| Parameters | Estimate (2.5–97.5th) |
|---|---|
| TS model | |
| $TS_0(cm) = \theta_{TS0} \times [1 + \theta_{NLSB} \times (NLSB - 2)] \times [1 + \theta_{NODB} \times (NODB - 2)]$ | $\theta_{TS0}$ = 6.04 (5.65–6.66)<br>$\theta_{NLSB}$ = 0.299 (0.208–0.363)<br>$\theta_{NODB}$ = 0.123 (0.06–0.23) |
| Kp ($wk^{-1}$) | 0.0103 (0.003–0.0104) |
| Slope (wk × AUC)$^{-1}$* | 0.00058 (0.00014–0.0067) |
| $K_R$ ($wk^{-1}$) | 0.0162 (0.013–0.129) |
| ISV_$TS_0$ (%) | 40 (33–48) |
| ISV_Kp (%) | 87 (82–176) |
| ISV_Slope (%) | 86 (80–202) |
| Residual error (log(cm)) | 0.276 (0.191–0.332) |
| OS model | |
| λ | 0.0126 (0.009–0.015) |
| β ($wk^{-1}$) = $\theta_\beta \times \theta_{ECOG}$ | $\theta_\beta$ = 1.63 (1.5–2.02)<br>$\theta_{ECOG(ECOG \geq 1)}$ = 1<br>$\theta_{ECOG(ECOG = 0)}$ = 0.433 (0.112–0.652) |
| γ ($(log(cm))^{-1}$) | 0.618 (0.419–1.02) |

Parameters are listed as estimates with 95% confidence intervals obtained from 500 bootstrap analyses in parenthesis. Estimates of inter-subject variability (ISV) are shown as coefficients of variation. $\theta_{NLSB}$, $\theta_{NODB}$, $\theta_{ECOG}$, are parameters quantifying the covariate effects of the NLSB and NODB on $TS_0$, and the ECOG status on the parameter $\beta$.

* Units of AUC of gemcitabine metabolite in white blood cells (wk·picomol/$10^6$ cells).

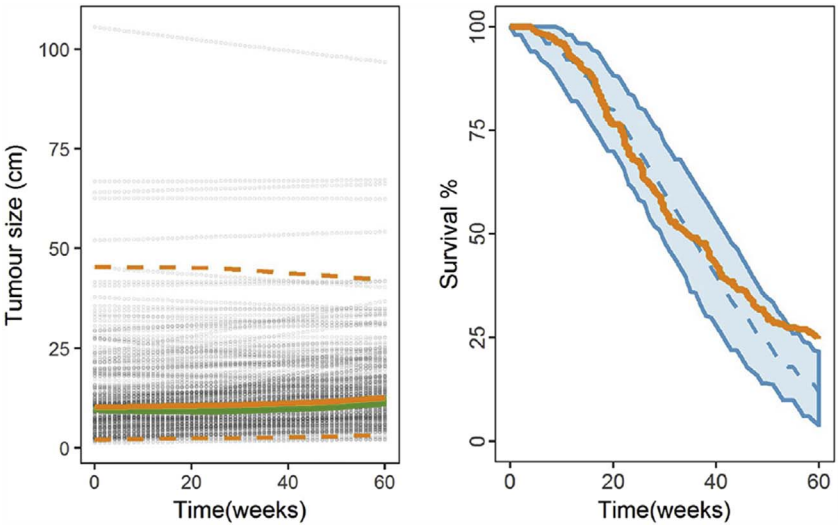


**Fig. 3.** External model validation. Left panel. Points represent the individual TS profiles associated with the external dataset summarized as 5th, 50th, and 95th percentiles (lines in orange). The area in green represents the 90% prediction interval of the 50th percentile of the simulated TS profiles using the current model. Right panel. Kaplan Meier plot of OS probability corresponding to the validation dataset (line in orange), and the 95% prediction interval calculated from the 500 simulated studies (blue shaded area).Dashed blue line represents the median simulated OS probability curve. (For interpretation of the references to colour in this figure legend, the reader is referred to the web version of this article.)

rest from treatment) incorporating or not resistance into treatment. Over 6 chemotherapy cycles, tolerance development elicits a maximal tumour regression (($TS_0$-TS(t))/$TS_0$) of 3.33% and maximal tumour growth inhibition (($TS_{untreated}$(t)-TS(t))/$T_{untreated}$(t)) of 22.3%, compared to the 10.28% and 29.9% produced in absence of tolerance, respectively. Thus, emerging resistance decreases $E_{drug}$ on each drug administration, reaching a 50% decrease during the 5th chemotherapy cycle.

## 4. Discussion

The paradigm represented by sequentially linking drug exposure, bio-, and/or surrogate marker(s), and clinical response (progression free survival, OS) has been applied successfully over the last decade to optimize the development of new anticancer agents and improve patient care in the clinical setting. Starting from the work carried out in NSCLC (Wang et al., 2009), models using TS as a predictor variable of clinical response have been developed for various type of tumours such as colorectal (Claret et al., 2009), thyroid (Claret et al., 2010), breast (Bruno et al., 2012) and ovarian (Zecchin et al., 2016) cancer, providing oncologists with quantitative tools capable of predicting disease progression using early clinical data, enabling go/no-go decision making before Phase 3 trials are initiated.

It is noteworthy that the examples cited above, except for NSCLC, correspond to tumour types associated with median-high 5 year relative survival rates which range between 46 and 98% (Miller et al., 2016). However, for tumours with even poorer prognoses, such as advanced pancreatic cancer, the potential for these predictive modelling frameworks is yet to be fully understood.

Our study focuses on the development of a predictive model for the effects of gemcitabine administered as single agent to patients with advanced pancreatic cancer. Pancreatic cancer is reported to have the lowest 5-year relative survival rate (5%) in cancer diseases (Miller et al., 2016), with a median survival time of 6 months for advanced disease (Muniraj et al., 2013), values that are in accordance with our data (Fig. 1A, right panel).

From a methodological point of view, model development in the current context is associated with several complexities and challenges that have been fully taken into account in the current evaluation. For example: (i)The continuous (TS dynamics) and the non-continuous time-to-event (OS) responses were analysed simultaneously due to the informative characteristics of the drop-outs (Hu & Sale, 2003), and (ii) to achieve the objective of developing a predictive tool, the model for TS should reflect the main processes affecting tumour dynamics (drug effects, progression of the disease, and possibly tolerance/resistance to treatment). The proposed TS model indicates exponential growth in the absence of treatment or for patients not responding to gemcitabine, assuming the ideal conditions in which tumour cells have sufficient

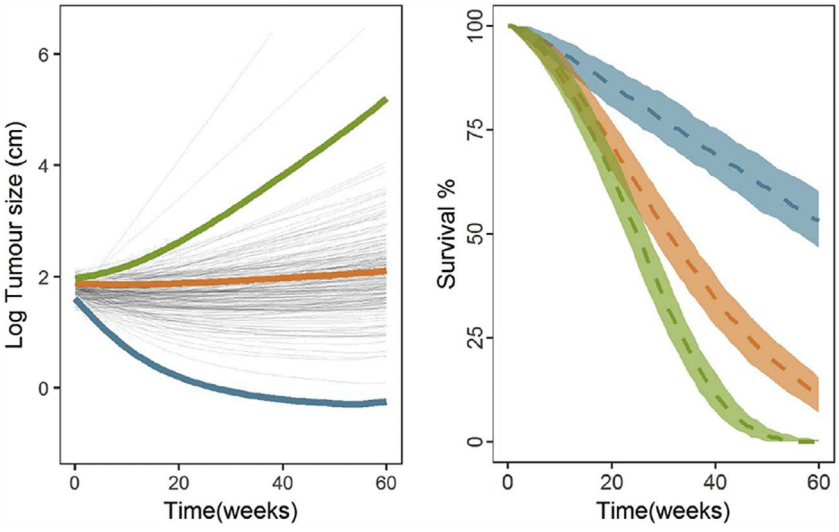


**Fig. 4.** Impact of TS profiles on the OS probability. Left panel. TS simulated profiles given the standard gemcitabine treatment schedule. Thin grey lines represent 200 TS simulated profiles, while thick green, orange and blue profiles represent disease progression, stable disease and response to treatment, respectively. Right panel. Kaplan Meier plots [lines (median); shaded areas (95% prediction intervals)] associated to TS profiles shown in left panel. (For interpretation of the references to colour in this figure legend, the reader is referred to the web version of this article.)

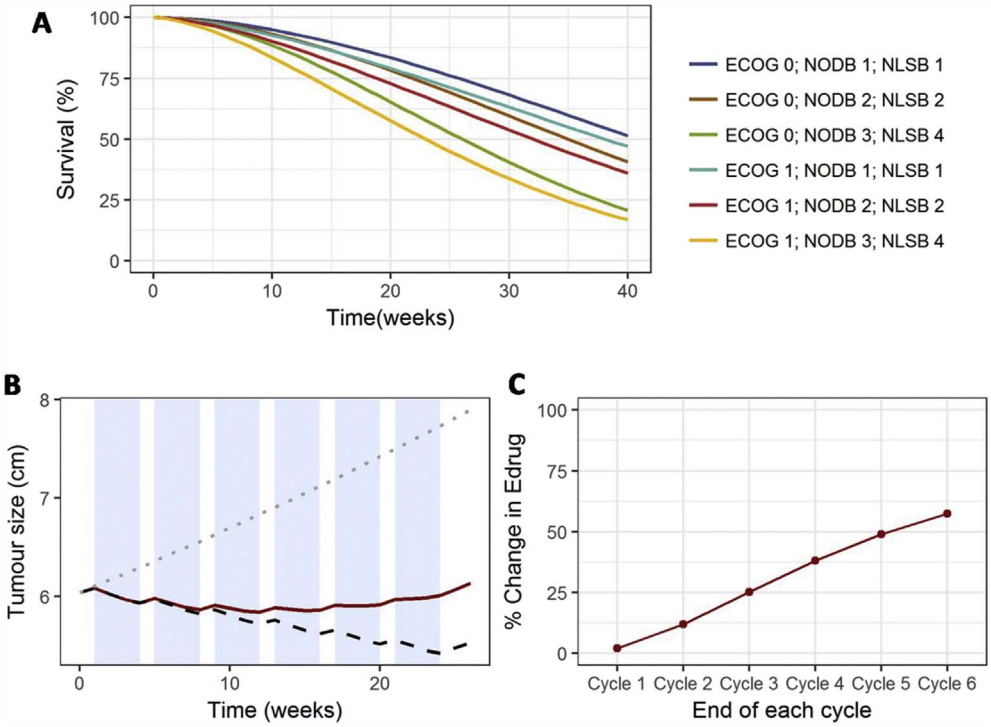


**Fig. 5.** Model exploration. A. OS probability profiles as a function of NLSB (number of tumour lesions at baseline), NODB (number of organs damaged with tumour lesions at baseline) and ECOG. B. Typical predicted tumour size for an untreated patient (points), and for two patients receiving 6 cycles of the standard treatment of gemcitabine (30 min i.v infusion of 1000 mg/m2 weekly ×3 followed by a week of rest from treatment) considering (solid line) or not (dashed line) the development of resistance. Each vertical area corresponds to a cycle of treatment. C. Represents the percentage of change in Edrug (see Eq. 2 in the text), at the end of each chemotherapy cycle.

nutrients to undergo continuous proliferation (Ribba et al., 2014). The model was able to characterize the data well, providing satisfactory results in terms of individual and population data (Fig. 2A). Resistance to treatment, far from being just a gemcitabine treatment-related phenomenon (Bergman et al., 2002; Binenbaum et al., 2015), has been well documented in oncology (Longley & Johnston, 2005). Of note, for the case of metastatic breast cancer patients treated with paclitaxel/gemcitabine combination therapy, emerging resistance occurs faster, with the mean tumour shrinkage rate dropping by half after 5.7 weeks (Tate et al., 2016) compared to the 20 weeks (Fig. 5B,C) for the current analysis. In contrast, for advanced and/or metastatic colorectal cancer patients treated with capecitabine or FU, the tumour shrinkage rate decrease by half in 13 and 16 weeks (Claret et al., 2009), respectively, slightly faster but similar to our case.

Whereas the use of a TS-derived metric [change from baseline predicted at a fixed time point (i.e, 8 weeks after the start of the treatment (Wang et al., 2009))] has been used to predict OS with the advantage of its simplicity, in our analysis the full predicted time profile of TS was used, which allows a more realistic characterization of the hazard profile to be obtained. Results from simulation exercise and represented graphically in Figs. 4 and 5 (top panel), reveal that TS exerted an impact on OS far beyond the statistical significant improvement in the fit. The impact of the NLSB and NODB, and ECOG status is much more reduced as can be noted in Fig. 5A. For example, the median predicted survival time for ECOG 0 and ≥1 in the case of two organs affected showing two lesions was 35 and 32 weeks, respectively. Neither tumour location, nor development of metastasis showed statistical significance on OS. Our results could be explained by the fact that patients from our analysis already presented advanced and/or metastatic disease at the time of being enrolled in the trial.

Recently a model relating TS with OS but with the limitation of not considering drug exposure as a predictor of TS dynamics was established for gemcitabine effects on pancreatic cancer (Wendling et al., 2016). We made use of the reported parameters to recreate virtual patients and externally validate our model (see Fig. 3). We emphasize the general need of integrating drug exposure for predictive population PKPD models, and in particular for the case of gemcitabine since clinical results suggest that the anti-tumour effects of gemcitabine are schedule dependent (Ciccolini et al., 2016).

One pending issue that could not be addressed in the current analysis was the identification of patient-related factors responsible for the high variability associated with the rate of tumour proliferation and drug effects (87 and 86%, respectively). Several studies suggest that the different rates of responses associated with gemcitabine treatment could in part be explained by individual genetic factors affecting, among other processes, the gemcitabine metabolism pathway (de Sousa Cavalcante & Monteiro, 2014), leading to different amounts of the active metabolite.

In conclusion, this joint modelling exercise predicts the efficacy of gemcitabine in terms of tumour growth inhibition and OS of patients with advanced pancreatic cancer. The analysis is expected to have an impact on the development of new anticancer drugs as our results indicate that phase II and III data share the same model structure and model parameter estimates. Therefore, the current modelling framework could be used for predicting late clinical outcome from early phase II data, optimizing the design of late phase clinical trials for advanced pancreatic cancer. It will also serve to optimize the standard treatment of pancreatic cancer patients receiving the drug of interest, predicting the likelihood of treatment success and assisting with the selection of dosing regimens.

Despite of the advanced stage of the disease, this analysis has identified a significant impact of TS on clinical response. This result encourages the development of a translational approach (Garcia-Cremades et al., 2016) based on recent semi-mechanistic tumour growth inhibition models developed in mice pancreatic and ovarian xenografts (Garcia-Cremades et al., 2017).

## Acknowledgements

The authors would like to thank Sonya Tate for providing assistance during the writing process.

This work is part of the Innovative Medicine Initiative (IMI) funded project Drug Disease Model Resources [DDMoRe (http://www.ddmore.eu/)] aiming to develop an interoperability framework including model repository to optimize model development. Support was received from the Innovative Medicines Initiative Joint Undertaking under grant

agreement no. 115156, resources of which are composed of financial contribution from the European Union's Seventh Framework Programme (FP7/2007-2013) and EFPIA companies' in kind contribution. The DDMORE project is also financially supported by contributions from Academic and SME partners.

Iñaki F Troconiz is an employee of the University of Navarra and Maria Garcia-Cremades is a Phd student from University of Navarra. Celine Pitou and Philip W Iversen are employees of Elli Lilly and Company.

## Appendix A. Supplementary data

Supplementary data to this article can be found online at https://doi.org/10.1016/j.ejps.2018.01.033.

## References


Bauer, R., 2011. NONMEM Users Guide: Introduction to NONMEM 7.2.0. ICON Development Solutions, Ellicott City.

Bender, B.C., Schindler, E., Friberg, L.E., 2015. Population pharmacokinetic-pharmacodynamic modelling in oncology: a tool for predicting clinical response. Br. J. Clin. Pharmacol. 79 (1), 56–71 (Jan).

Bergman, A.M., Pinedo, H.M., Peters, G.J., 2002. Determinants of resistance to 2′,2′-difluorodeoxycytidine (gemcitabine). Drug Resist. Updat. 5 (1), 19–33.

Bergstrand, M., Hooker, A.C., Wallin, J.E., Karlsson, M.O., 2011. Prediction-corrected visual predictive checks for diagnosing nonlinear mixed-effects models. AAPS J. 13 (2), 143–151 (Jun).

Binenbaum, Y., Na'ara, S., Gil, Z., 2015. Gemcitabine resistance in pancreatic ductal adenocarcinoma. Drug Resist. Updat. 23, 55–68 (Nov).

Bruno, R., Lindbom, L., Schaedeli Stark, F., Chanu, P., Gilberg, F., Frey, N., et al., 2012. Simulations to assess phase II noninferiority trials of different doses of Capecitabine in combination with docetaxel for metastatic breast cancer. CPT Pharmacometrics Syst. Pharmacol. 1, e19 (Dec 26).

Chen, X., Summers, R.M., Yao, J., 2013. Kidney tumor growth prediction by coupling reaction-diffusion and biomechanical model. IEEE Trans. Biomed. Eng. 60 (1), 169–173.

Ciccolini, J., Serdjebi, C., Peters, G.J., Giovannetti, E., 2016. Pharmacokinetics and pharmacogenetics of gemcitabine as a mainstay in adult and pediatric oncology: an EORTC-PAMM perspective. Cancer Chemother. Pharmacol. 78 (1), 1–12 (Jul).

Claret, L., Girard, P., Hoff, P.M., Van Cutsem, E., Zuideveld, K.P., Jorga, K., et al., 2009. Model-based prediction of phase III overall survival in colorectal cancer on the basis of phase II tumor dynamics. J. Clin. Oncol. 27 (25), 4103–4108.

Claret, L., Lu, J.F., Sun, Y.N., Bruno, R., 2010. Development of a modeling framework to simulate efficacy endpoints for motesanib in patients with thyroid cancer. Cancer Chemother. Pharmacol. 66 (6), 1141–1149 (Nov).

Collett, D., 1952. Modelling Survival Data in Medical Research.

Fuchs, C.S., Azevedo, S., Okusaka, T., Van Laethem, J.-L., Lipton, L.R., Riess, H., et al., 2015. A phase 3 randomized, double-blind, placebo-controlled trial of ganitumab or placebo in combination with gemcitabine as first-line therapy for metastatic adenocarcinoma of the pancreas: the GAMMA trial. Ann. Oncol. 26 (5), 921–927 (May).

Garcia-Cremades, M., Pitou, C., Iversen, W.P., Troconiz, F.I., 2016. A comparison of different model-based approaches to scale preclinical to clinical tumour growth inhibition in gemcitabine-treated pancreatic cancer. In: PAGE 25 (2016) Abstr 5704, . [www.page-meeting.org/?abstract=5704].

Garcia-Cremades, M., Pitou, C., Iversen, P.W., Troconiz, I.F., 2017. Characterizing gemcitabine effects administered as single agent or combined with carboplatin in mice pancreatic and ovarian cancer xenografts: a Semimechanistic pharmacokinetic/pharmacodynamics tumor growth-response model. J. Pharmacol. Exp. Ther. 360 (3), 445–456 (Mar).

Hogea, C., Davatzikos, C., Biros, G., 2008. An image-driven parameter estimation problem for a reaction-diffusion glioma growth model with mass effects. J. Math. Biol. 56 (6), 793–825.

Hu, C., Sale, M.E., 2003. A joint model for nonlinear longitudinal data with informative dropout. J. Pharmacokinet. Pharmacodyn. 30 (1), 83–103 (Feb).

Konukoglu, E., Clatz, O., Menze, B.H., Stieltjes, B., Weber, M.A., Mandonnet, E., et al., 2010. Image guided personalization of reaction-diffusion type tumor growth models using modified anisotropic eikonal equations. IEEE Trans. Med. Imaging 29 (1), 77–95.

Le, N., Sund, M., Vinci, A., 2016. Prognostic and predictive markers in pancreatic adenocarcinoma. Dig. Liver Dis. 48 (3), 223–230 (Mar).

Lindbom, L., Ribbing, J., Jonsson, E.N., 2004. Perl-speaks-NONMEM (PsN)—a Perl module for NONMEM related programming. Comput. Methods Prog. Biomed. 75 (2), 85–94.

Liu, Y., Sadowski, S.M., Weisbrod, A.B., Kebebew, E., Summers, R.M., Yao, J., 2014. Patient specific tumor growth prediction using multimodal images. Med. Image Anal. 18 (3), 555–566.

Longley, D.B., Johnston, P.G., 2005. Molecular mechanisms of drug resistance. J. Pathol. 205 (2), 275–292 (Jan).

Menze, B.H., Van Leemput, K., Honkela, A., Konukoglu, E., Weber, M.-A., Ayache, N., et al., 2011. A generative approach for image-based modeling of tumor growth. In: Székely, G., Hahn, H.K. (Eds.), Information Processing in Medical Imaging: 22nd International Conference, IPMI 2011, Kloster Irsee, Germany, July 3–8, 2011 Proceedings. Berlin, Heidelberg. Springer, Berlin Heidelberg, pp. 735–747.

Miller, K.D., Siegel, R.L., Lin, C.C., Mariotto, A.B., Kramer, J.L., Rowland, J.H., et al., 2016. Cancer treatment and survivorship statistics, 2016. CA Cancer J. Clin. 66 (4), 271–289 (Jul).

Mini, E., Nobili, S., Caciagli, B., Landini, I., Mazzei, T., 2006. Cellular pharmacology of gemcitabine. Ann. Oncol. 17 (Suppl. 5), v7–12 (May 1).

Moore, M., 1996. Activity of gemcitabine in patients with advanced pancreatic carcinoma. A review. Cancer 78 (3 Suppl), 633–638 (Aug 1).

Muniraj, T., Jamidar, P.A., Aslanian, H.R., 2013. Pancreatic cancer: a comprehensive review and update. Dis. Mon. 59 (11), 368–402 (Nov).

Neoptolemos, J.P., Stocken, D.D., Friess, H., Bassi, C., Dunn, J.A., Hickey, H., et al., 2004. A randomized trial of chemoradiotherapy and chemotherapy after resection of pancreatic cancer. N. Engl. J. Med. 350 (12), 1200–1210 (Mar 18).

Nyberg, J., Karlsson, K.E., Jönsson, S., Simonsson, U.S.H., Karlsson, M.O., Hooker, A.C., 2014. Simulating large time-to-event trials in NONMEM. In: PAGE 23 (2014) Abstr 3166, . [www.page-meeting.org/?abstract=3166].

Oettle, H., Arnold, D., Hempel, C., Riess, H., 2000. The role of gemcitabine alone and in combination in the treatment of pancreatic cancer. Anti-Cancer Drugs 11 (10), 771–786 (Nov).

Perkhofer, L., Ettrich, T.J., Seufferlein, T., 2014. Pancreatic cancer: progress in systemic therapy. Gastrointest. tumors 1 (4), 167–179 (May).

Ribba, B., Holford, N.H., Magni, P., Troconiz, I., Gueorguieva, I., Girard, P., et al., 2014. A review of mixed-effects models of tumor growth and effects of anticancer drug treatment used in population analysis. CPT Pharmacometrics Syst. Pharmacol. 3, e113 (May 7).

Ruess, D.A., Görgülü, K., Wörmann, S.M., Algül, H., 2017. Pharmacotherapeutic management of pancreatic ductal adenocarcinoma: current and emerging concepts. Drugs Aging 1–27.

Schober, M., Javed, M.A., Beyer, G., Le, N., Vinci, A., Sund, M., et al., 2015. New advances in the treatment of metastatic pancreatic cancer. Digestion 92 (3), 175–184.

de Sousa Cavalcante, L., Monteiro, G., 2014. Gemcitabine: metabolism and molecular mechanisms of action, sensitivity and chemoresistance in pancreatic cancer. Eur. J. Pharmacol. 741, 8–16 (Oct 15).

Tate, S.C., Andre, V., Enas, N., Ribba, B., Gueorguieva, I., 2016. Early change in tumour size predicts overall survival in patients with first-line metastatic breast cancer. Eur. J. Cancer 66, 95–103 (Oct).

Tham, L.S., Wang, L., Soo, R.A., Lee, S.C., Lee, H.S., Yong, W.P., et al., 2008. A pharmacodynamic model for the time course of tumor shrinkage by gemcitabine + carboplatin in non-small cell lung cancer patients. Clin. Cancer Res. 14 (13), 4213–4218 (Jul 1).

Toschi, L., Finocchiaro, G., Bartolini, S., Gioia, V., Cappuzzo, F., 2005. Role of gemcitabine in cancer therapy. Future Oncol. 1 (1), 7–17 (Feb).

Wang, Y., Sung, C., Dartois, C., Ramchandani, R., Booth, B.P., Rock, E., et al., 2009. Elucidation of relationship between tumor size and survival in non-small-cell lung cancer patients can aid early decision making in clinical drug development. Clin. Pharmacol. Ther. 86 (2), 167–174 (Aug).

Wendling, T., Mistry, H., Ogungbenro, K., Aarons, L., 2016. Predicting survival of pancreatic cancer patients treated with gemcitabine using longitudinal tumour size data. Cancer Chemother. Pharmacol. 77 (5), 927–938 (May).

Zecchin, C., Gueorguieva, I., Enas, N.H., Friberg, L.E., 2016. Models for change in tumour size, appearance of new lesions and survival probability in patients with advanced epithelial ovarian cancer. Br. J. Clin. Pharmacol. 82 (3), 717–727 (Sep).

Zhang, L., Sinha, V., Forgue, S.T., Callies, S., Ni, L., Peck, R., et al., 2006. Model-Based Drug Development: The Road to Quantitative Pharmacology. J. Pharmacokinet. Pharmacodyn. 33 (3), 369 (Jul).